Laser and Particle Beams (2001), *19*, 345–353. Printed in the USA.

Kinetic effects in *z* pinches

M.G. HAINES
Blackett Laboratory, Imperial College, London SW7 2BW, United Kingdom
(Received 22 May 2000; Accepted February 2001)

Abstract

Both dynamic and equilibrium *z* pinches are mostly described, whether in theory or in simulation, by conventional magnetohydrodynamic (MHD) fluid equations. However there are several key phases in *z*-pinch behavior when kinetic effects are important. Runaway electrons can occur close to the axis especially in an $m = 0$ neck or during the subsequent disruption. Large ion-Larmor orbits can, if sufficiently collisionless, lead to stabilizing effects. During a disruption, ion beams can be produced. For deuterium discharges, the interaction of an ion beam with the ambient plasma can lead to a significant neutron yield. If the drift velocity of the current-carrying electrons exceeds a threshold for generating microinstabilities (lower-hybrid or ion-acoustic instabilities), this leads to anomalous resistivity. This can occur not only during a disruption, but also in the low-density (usually outer) plasma boundary of an equilibrium or dynamic pinch. Related to this is the open question of whether current reconnection can occur in fully developed magneto-Rayleigh–Taylor instabilities in the low-density coronal plasma. Two other kinetic effects are new to *z* pinches. First, there are the collisions of low-density energetic ions from a wire array as they pass close to the axis to form a precursor plasma. Second, there is the possible erosion and ablation of wire cores in the necks of $m = 0$ coronal current-carrying plasma by flux-limited heat flow with its attendant deviation from a Maxwellian of the isotropic part of the distribution function.

1. INTRODUCTION

Kinetic effects can play an important role in any plasma that is insufficiently collisional so that there are significant departures from a Maxwellian distribution. Such departures occur, for example, when large electric fields or temperature gradients are present. Linear transport theory such as developed by Spitzer and Härm (1953) for zero magnetic field, **B**, or by Braginskii (1958) for $\mathbf{B} \neq 0$ is strictly valid only for arbitrarily small thermodynamic fluxes and forces. In the case of a finite electric field, it is possible for electrons to grow in velocity into a runaway regime. If the electrons are well magnetized, $\omega_{ce}\tau_{ei} \gg 1$, then runaway cannot occur in the plane perpendicular to the magnetic field. Here, ω_{ce} is the electron cyclotron frequency and τ_{ei} is the electron–ion collision time. In this case, the runaway electron effect is confined to the axis of a *z* pinch where the magnetic field is zero.

It is generally assumed that in the fast, high-density *z* pinches currently being studied (see, e.g., Matzen, 1997) that the line density of ions, N_i, and of electrons, ZN_i, where Z is the mean charge number, is so high that mean drift velocities are very low compared to thermal velocities or the sound speed, C_s, that conventional MHD theory applies together with linear transport theory.

However we will find regions in space and phases in time when this is not so, and kinetic effects are important.

In Section 2 we will briefly review the standard MHD theory and linear transport theory, and discuss the limits of applicability. In Section 3 we will consider when runaway electrons will occur. It is important here to distinguish off-axis guiding center orbits and the snake-like singular orbits in the vicinity of the magnetic axis (Haines, 1978), and especially to consider the occurrence of runaway electrons at the time of a disruption caused at the neck of an $m = 0$ MHD sausage instability. Such MHD instabilities can, however, be mollified by similar orbit considerations of the ions. In Section 4 the stabilizing effect of large ion-Larmor orbits will be reviewed.

A *z* pinch can be formed from a wire or solid fiber or indeed from an array of wires, when after a period of heating and phase transitions to liquid and vapor in the case of a metal, a coronal plasma is formed following surface breakdown and ionization. Because of its higher electrical conductivity, the current switches to this plasma. Though forming

Address correspondence and reprint requests to: M.G. Haines, Blackett Laboratory, Imperial College, London SW7 2BW, United Kingdom. E-mail: m.haines@ic.ac.uk

only a small fraction of the total mass, it carries nearly all the current. However as the magnetic pressure rises relative to the plasma pressure, this plasma tends to go unstable to $m = 0$ instabilities (Beg *et al.*, 1997). Simulations by Chittenden *et al.* (1999) show this and, furthermore, identify that the observed bright X-ray emitting regions are rings of dense plasma in the necks in which heat flux is strongly flowing to the dense core. In this region, the temperature gradient can be so strong that nonlinear heat flow might arise, similar to that found in the laser–plasma approach to inertial confinement fusion. This will be discussed in Section 5. Indeed a recent analytic model (M.G. Haines, in prep.) shows that flux-limited heat flow in the magnetically compressed plasma in each neck leads to a time consistent with experiment to convert the wires to a plasma. It also is effective in clamping the electron temperature of the coronal plasma, so that both $\omega_{ce}\tau_{ei}$ and the magnetic Reynolds' number R_m are less than unity. The first condition, however, will permit runaway electrons and ion-acoustic turbulence to build up, while the second condition allows the plasma in the $m = 0$ bulges to leave the current and magnetic field region and to become force-free flares. In a wire array, the effect of the global magnetic field is to convert these flares into radially inward flowing low-density field-free plasma jets. In Section 6, we consider how ion–ion collisions can cause these radially converging and relatively collisionless plasma ions to accumulate on the axis of the wire-array as a stable column of precursor plasma as observed by Aivazov *et al.* (1988) and Lebedev *et al.* (1999).

In Section 7, we review the triggering of microturbulence, both lower-hybrid and ion-acoustic, which leads to anomalous resistivity. This effect could be important at an early phase of coronal plasma formation; also in the low-density boundary regions of the plasma; and, most important, in the necks of an $m = 0$ instability as the line density drops and the mean drift velocity increases. Section 8 deals with the disruption itself and a discussion of the many and controversial theories to explain the occurrence of ion beams as well as electron beams, the former in turn leading to neutron production if deuterium is employed as the ion species.

2. DEVIATIONS FROM EQUILIBRIUM

Considering first the electron plasma, the Fokker–Planck equation can be expanded in a tensor expansion (Johnston, 1960) so that the distribution function is of the form

$$f = f_0 + \frac{\underline{f}_1 \cdot \underline{v}}{v} + \frac{\underline{\underline{f}}_2 : \underline{v}\underline{v}}{v^2} + \ldots. \tag{1}$$

In the rest frame of the ions and for a Lorentz plasma (i.e., neglecting electron–electron collisions, valid for large atomic Z), the dimensionless vector $\underline{F}_1$ in steady-state is related to the Maxwellian $f_0 = f_m$ by (Epperlein & Haines, 1986; Haines, 1992)

$$\underline{F}_1 = \frac{F_m}{1 + \Omega^2 V^{2n}} \times (-V^{n+1}\underline{e} - \Omega V^{2n+1}\underline{b} \times \underline{e} - V^{n+2}\underline{t} - \Omega V^{2n+3}\underline{b} \times \underline{t}), \tag{2}$$

where $\underline{e}$ and $\underline{t}$ are the dimensionless thermodynamic forces,

$$\underline{e} = \frac{2e\underline{E}}{m_e v_T \nu_T} + \frac{v_T}{\nu_T}\frac{\nabla P_e}{P_e} - \frac{5}{2}\frac{v_T}{\nu_T}\frac{\nabla T_e}{T_e} \tag{3}$$

$$\underline{t} = \frac{v_T}{\nu_T}\frac{\nabla T_e}{T_e}, \tag{4}$$

and the other quantities are defined by $F = 4\pi v_T^3 f/n$, $V = v/v_T$, $v_T = (2T_e/m_e)^{1/2}$, $\underline{b} = \mathbf{B}/|\mathbf{B}|$, $\nu_T = 3\sqrt{\pi}/(4\tau_{ei})$, and $\Omega = \omega_{ce}/\nu_T$ where the electron–ion collision time and Maxwellian f_m are

$$\tau_{ei} = \tfrac{3}{4}(4\pi\epsilon_0)^2 m_e^{1/2} T_e^{3/2}/(2^{1/2}\pi^{1/2} n_i Z^2 e^4 \ln\Lambda) \tag{5}$$

and

$$f_m = \frac{n}{\pi^{3/2} v_T^3}\exp\left(-\frac{v^2}{v_T^2}\right). \tag{6}$$

Here the collision frequency for an electron of dimensionless velocity V is $v_T V^{-n}$, and for a fully ionized plasma $n = 3$. It is from this velocity dependence of the collision frequency that (a) runaway electrons can occur, and (b) in linear transport theory the thermoelectric term and the Nernst term (proportional to $\underline{b} \times \nabla T_e$) arise in Ohm's law and the Ettingshausen term (a heat flux in the direction of $\mathbf{J} \times \mathbf{B}$, $\mathbf{J}$ being the current density) arises in the heat flux equation. Chittenden and Haines (1993) showed how in a z pinch, the large heating per electron in the outer, low density region of the z pinch did not lead to a thermal instability; rather the Ettingshausen inward heat flow (associated with an E/B inward drift of the hotter, less collisional, electrons) removes this excess energy, while the Nernst effect ensures an inward convection of the magnetic field (and associated current) through it being more frozen to the hotter electrons.

The condition for onset of runaway electrons was found by Dreicer (1960) for electrons with a velocity V such that

$$V = \frac{v}{v_T} \geq \left(\frac{v_T}{v_D}\right)^{1/2}, \tag{7}$$

where the classical drift velocity v_D is given by

$$0.381\,\frac{v_D}{v_T} = \frac{eE_\phi}{m\nu_T v_T} \tag{8}$$

https://doi.org/10.1017/S0263034601193092 Published online by Cambridge University Press

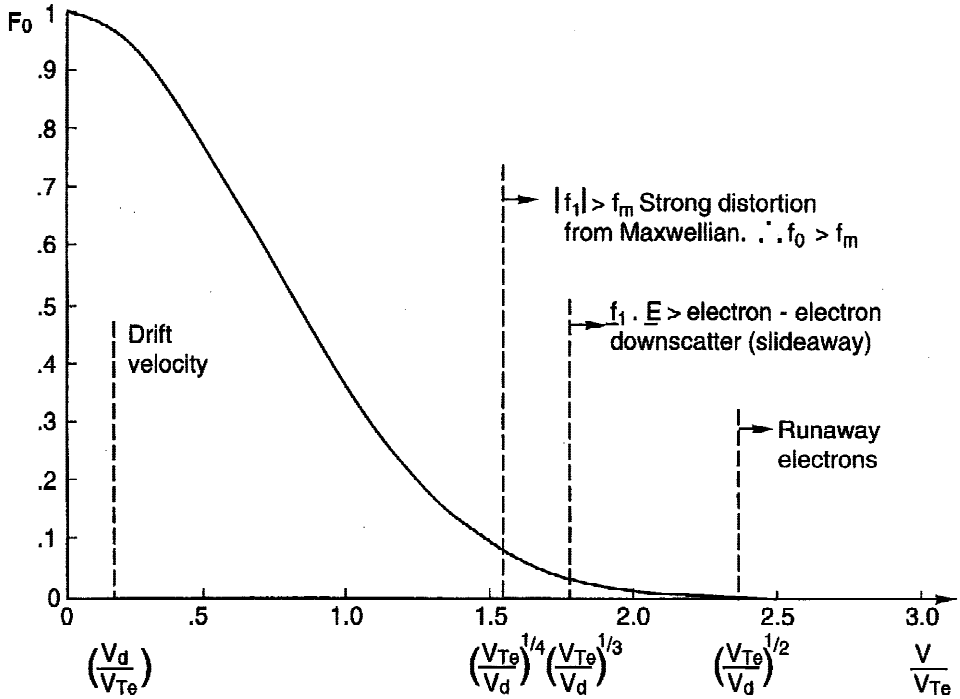

Fig. 1. A sketch of a Maxwellian distribution $F_0 = \exp(-v^2/v_{T0}^2)$ versus v/v_{T0}, showing the values of v/v_{T0}: (i) $(v_{T0}/v_d)^{1/4}$ at which there is a strong distortion of F_0 from a Maxwellian; (ii) $(v_{T0}/v_d)^{1/3}$ at which the Joule heating balances the electron–electron downscatter; and (iii) $(v_{T0}/v_d)^{1/2}$ at which runaway electrons will occur. The value of v_d/v_{T0} is also indicated, where v_D is the mean drift velocity of the electrons relative to the ions (Haines, 1996).

for a $Z = 1$ plasma. On the other hand, the condition for $F_1(V) > F_m(V)$ for the case $\underline{t} = 0$, $n = 3$, $\Omega = 0$ is

$$V = \frac{v}{v_\tau} \geq \left(\frac{v_\tau}{v_D}\right)^{1/4}, \tag{9}$$

which is a much lower velocity. Thus a significant departure from a Maxwellian f_0 will occur for V approaching and greater than this critical value. An intermediate critical value of $V = (v_T/v_D)^{1/3}$ was found by Dreicer (1960) above which the Joule heating exceeded the downscatter of electron energy by electron–electron collisions. These critical velocities are illustrated in Figure 1 (taken from Haines, 1996). A similar condition for $|\underline{F}_1| > F_m$ exists for temperature gradients when nonlinear heat flow (Sect. 5) applies.

To consider large ion Larmor radius effects, the tensor $\underline{\underline{f}}_2$ [Eq. (1)] has to be evaluated.

3. SINGULAR ORBITS AND RUNAWAYS

Following Haines (1978), the radial pressure balance for electrons can be written as

$$0 = -n_e e E_r + n_e e v_{ez} B_\theta + (P_{\|e} - P_{\perp e})/r - \partial P_{\perp e}/\partial r. \tag{10}$$

On rearranging to give

$$v_{ze} = \frac{1}{n_e e r}\frac{\partial}{\partial r}\left(\frac{r P_{\perp e}}{B_\theta}\right) + \frac{P_{\perp e}}{n_e e B_\theta^2}\frac{\partial B_\theta}{\partial r} - \frac{P_{\|e}}{n_e e B_\theta r} + \frac{E_r}{B_\theta}, \tag{11}$$

it is seen that the center-of-mass velocity of the electrons in the z-direction is equal to the diamagnetic velocity plus the three guiding centre components due to ∇B, curvature and $\mathbf{E} \times \mathbf{B}/B^2$ drifts. On multiplying by $-\int n_e e r 2\pi\, dr$ and integrating over the pinch it is found that the current I is the sum of the singular current for electrons I_{se} and the current due to off-axis guiding center motion, where

$$I_{se} = -2\pi\left[\frac{r P_{\perp e}}{B_\theta}\right]_{r=0} = -\frac{4\pi}{\mu_0}\left[\frac{P_{\perp e}}{J_z}\right]_{r=0}. \tag{12}$$

I_{se} is the current caused by electrons of thermal velocity that are within one Larmor radius of the axis, and travel on average in the direction from the cathode towards the anode, that is,

$$I_{se} = -n_e e v_{\perp e} \pi R_e^2, \tag{13}$$

where

$$R_e = \frac{v_{\perp e}}{\omega_{ce}(R_e)} = \frac{2 m_e v_{\perp e}}{e \mu_0 I_z(r=0)} \tag{14}$$

and $P_{\perp e}$ is $\frac{1}{2} n_e m_e v_{\perp e}^2$.

https://doi.org/10.1017/S0263034601193092 Published online by Cambridge University Press

There is a similar singular current I_{si} for ions that move with snake-like orbits in the opposite direction, given by

$$I_{si} = \frac{4\pi}{\mu_0}\left[\frac{P_{\perp i}}{J_z}\right]_{r=0}. \tag{15}$$

If the axial ion center of mass velocity is zero, then I_{si} is equal and opposite to the current associated with the mean guiding center motion of the ions. For the special case of $Z = 1$ isotropic pressure and $T_i = T_e$, it follows that I_{si} is equal to I_{se} and each is half of the total current. If the plasma is relatively collisionless ($\omega_{ce}\tau_{ei} \gg 1$), then the singular orbits are important and can lead to runaway electrons and energetic ion beams (see Sect. 8), especially at a disruption.

Figure 2, taken from Chittenden and Haines (1993), shows how a hot electron is filtered towards the axis with a E_z/B_θ guiding center velocity as it forms part of the radially inward Ettingshausen heat flow. It then converts to a singular electron orbit and is prone to run away in the applied E_z field if Eq. (7) is satisfied.

It should be pointed out that the off-axis guiding center particles interlink orbits with the singular particle orbits, that is, for the electrons, the diamagnetism redistributes their effect so that the current density can be small on the axis even though half the current can be carried by the singular electrons.

However, if there are no or insufficient off-axis electrons, as in the case of a diode, then I_z becomes $-n_e e v_{ze}$ and $P_{\perp e} = n_e m_e v_{ze}^2$ so that I_{se} becomes Alfvén–Lawson limiting current, I_A given by

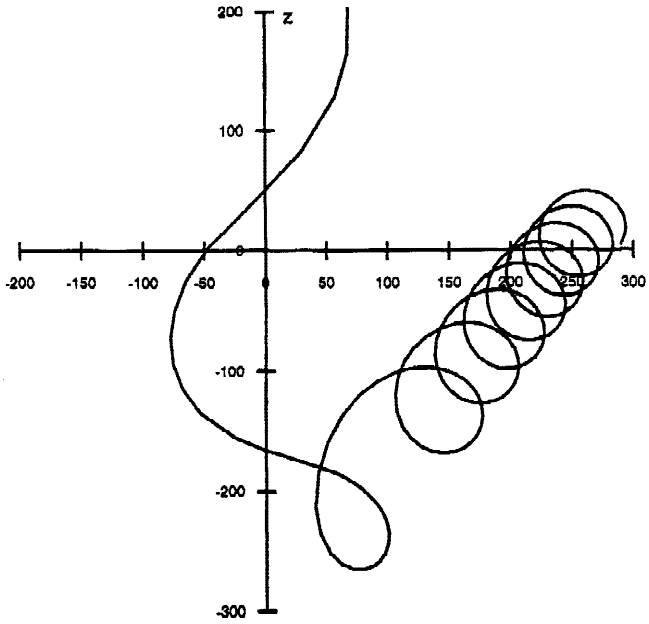

Fig. 2. Trajectory of an electron with five times the thermal energy ($v_r = v_z$, $v_\theta = 0$) in r–z space in micrometers (Chittenden & Haines, 1993).

$$I_A = \frac{4\pi}{\mu_0}\frac{m_e}{e}v_{\perp e} \tag{16}$$

or, relativistically,

$$I_A = 17{,}000\gamma\beta \text{ (Amperes)} \tag{17}$$

where $\beta = v_{\perp e}/c$ and $\gamma = (1-\beta^2)^{-1/2}$. It is unlikely that a runaway current greater than this can penetrate through and leave the anode of a z pinch.

4. LARGE ION-LARMOR RADIUS AND STABILITY

As shown by Haines and Coppins (1991) in a classification of stability regimes for the z pinch, there is a regime in $I^4a - N$ space where $\omega_{ci}\tau_i > 1$ and $a_i/a > 0.1$ where ω_{ci} is the ion cyclotron frequency, τ_i the ion–ion collision time and a_i/a is the ratio of the ion-Larmor radius to the pinch radius. Incidentally, this is the regime for a D-T fusion z pinch.

Linear and nonlinear stability has been studied by numerically solving the Vlasov equation for the ions usually with the electrons treated as a cold Hall fluid background, freezing them to the magnetic field. The growth rates are complex. The Vlasov model naturally allows anisotropy through f_2 to develop and it can be used for arbitrarily large ion-Larmor radius. Arber *et al.* (1994) show that for the $m = 0$ mode, there is a considerable reduction in the growth rate as compared to the Chew–Goldberger–Low (CGL) ordering at zero Larmor radius. Both a linearized initial value code, FIGARO, and a variational code show that for a parabolic density profile, the growth rate has a minimum of 0.3 the CGL model at $a_i/a \cong 0.2$. The reason for increased growth at larger a_i is not fully understood, but is probably because as the ion-Larmor radius increases, the time to complete an orbit becomes comparable to the MHD growth time, and so there is less time for kinetic smoothing of the MHD mode. The variational code has also explored the $m = 1$ mode, and it is interesting to find that there is a more marked stabilizing effect here with a 80% reduction in growth rate at $a_i/a \cong 0.2$. (Arber *et al.*, 1995).

There is good experimental evidence (Davies *et al.*, 2001; Haines *et al.*, 1990) for a reduction in growth rate under large ion-Larmor radius conditions. Unfortunately it would seem from Arber (1996) that nonlinearly, the $m = 0$ instability continues to grow exponentially without saturation, presumably until the plasma column disrupts.

5. FLUX-LIMITED HEAT FLOW

During the evolution of a solid fiber to form a surrounding coronal plasma that carries most of the current, there is a boundary between the plasma and the expanding core where a steep temperature gradient can occur. Indeed, it is the heat supplied through this temperature gradient that could be the main source of energy for ablating or eroding the core and

https://doi.org/10.1017/S0263034601193092 Published online by Cambridge University Press

converting each layer to an ionized plasma, though there will also be both the Joule heating by the residual current in the core and the internal energy stored in the core. A steep gradient is required to transfer sufficient energy, and under this condition the heat flux becomes nonlinear, f_0 departs from a Maxwellian distribution, and a full Fokker–Planck calculation is required such as carried out for laser-heated plasmas for inertial confinement fusion by Bell *et al.* (1981).

Fortunately it is quite often the case that a crude flux-limiter f where $f = 0.1$ to 0.2 gives adequate representation, so that the heat flux q can be given an approximate upper limit of $fn_e m_e v_{Te}^3/2\sqrt{2}$ where $v_{\tau e}^2 = 2T_e/m_e$. A comparison of this approximation, another nonlocal approximation based on a convolution or Green's function approach, and a Fokker–Planck solution was published by Holstein *et al.* (1986) for the case of heat flux from a laser-heated plasma (at the critical surface) to the near solid density ablation surface.

It is perhaps pertinent to consider the particular case of $\underline{t} \neq 0$, $e = -\frac{5}{2}\underline{t}$, $\Omega = 0$ in Eq. (2). The critical velocity at which F_1 is equal to F_m was employed by Shvarts *et al.* (1981) as the upper limit to the heat flux moment equation. This critical velocity is $(L_T/\lambda_{mfp})^{1/6} = |\underline{t}|^{-1/6}$ where L_T is $T_e/|\nabla T_e|$. Linear transport theory, if defined as valid if 90% of the Spitzer heat flux occurs for electrons with velocity less than the critical velocity, gives a critical velocity of $3v_{Te}$. For steeper temperature gradients, it is a good approximation to take the geometric mean of the Spitzer heat flow and the heat flux calculated by limiting the integration to the critical velocity in order to obtain agreement with Fokker–Planck calculations.

6. ION–ION COLLISIONS

Ion–ion collisions are important in two phases of a wire array implosion. The first is during the formation of the precursor column, while the second is at stagnation when the kinetic energy of the imploding ions, perhaps 70–1000 keV, is randomized by viscosity to give an ion temperature. This, in turn, leads on to equipartition to the electrons, further ionization and the observed intense X-ray emission. The second process can be very fast due to the high stagnation density.

Of more novel interest is the first process, because the ion mean-free-path can be large compared to the dimensions of the inner low-density plasma. Once the density on axis rises above a critical value, then ion–ion collisions begin to dominate and a stagnated plasma column appears on the axis. Prior to this, the ion streams interpenetrate each other.

The more general problem of collision between counter-streaming ions of charge Z and Z' and of velocity v and v^1, gives a collision time τ_{ii} for the scattering of an ion of charge Z:

$$\tau_{ii}^1 = \frac{3}{4}\frac{m_i^{1/2}\epsilon^{3/2}(4\pi\epsilon_0)^2}{\sqrt{2\pi}n_i^1 Z^2 Z^{12} e^{5/2}\ln\Lambda_{ii'}}, \tag{18}$$

where

$$\ln\Lambda_{ii'} = \ln(\lambda_{De}/\lambda_{0ii'}) = 49.94 - \ln\left(\frac{n_e^{1/2}}{T_e^{1/2}}\cdot\frac{\mu+\mu^1}{\mu\mu^1}\cdot\frac{ZZ^1}{\beta_D^2}\right), \tag{19}$$

$\epsilon = \frac{1}{2}m_i v_D^2/e$, $v_D = v + v^1 = \beta_D c$, $\mu = m_i/m_p$, and $\mu^1 = m_{i^1}/m_p$. The ion relative energy, ϵ, is in electron volts, and in $\ln\Lambda_{ii}$, the maximum impact parameter is determined by electron screening, assuming that the electron thermal speed is greater than v_D; however the minimum impact parameter λ_{0ii^1} is for ion–ion 90° deflections. In Eq. (18) the units are m^{-3} for n_e and eV for τ_e.

Considering like-like species of aluminium plasma with $v_D = 4\times10^5$ ms^{-1}, $n_i = 6\times10^{24}$ m^{-3} (10^{-4} of solid density), $T_e = 30$ eV, the Thomas–Fermi ionization level is Z $(=Z^1) = 8$, $\ln\Lambda_{ii} = 7.28$, and $\epsilon = 22.5\times10^3$ eV. Then τ_{ii} is 1.4×10^{-9} s and the mean-free-path of the ions in the laboratory frame where $v = \frac{1}{2}v_D$ is 0.29 mm. Thus these conditions are on the margins of being collisional. In the Imperial College MAGPIE experiment, a precursor plasma column is formed of radius a few mean-free-paths.

On repeating this calculation for tungsten plasma with $v_D = 4\times10^5$ ms^{-1}, $n_i = 6.3\times10^{24}$ m^{-3} ($10^{-4}\times$ solid density), $\tau_e = 10$ eV, this gives $Z = 7$, $\ln\Lambda_{ii} = 7.57$, and $\epsilon = 38.4\times10^3$ eV. But now τ_{ii} is 1.3×10^{-8} s and the mean-free-path is 2.6 mm, both an order of magnitude larger. Therefore interpenetration of the tungsten streams will occur. Indeed in the experiment, a narrow plasma column only appears when another phenomenon, namely radiation cooling or collapse occurs, so increasing the plasma density through contraction under dynamic pressure effects.

Experimental evidence from end-on laser interferometry attests to more collisional behavior from the interaction of adjacent inward moving streams as they converge towards the axis in aluminum plasmas; in contrast, tungsten streams have no shock-like structures and no sharp density variation occurs.

When a tungsten wire array plasma streams to the axis and interacts with a plastic foam cylinder on the axis, for a larger tungsten streaming velocity v of 4×10^5 ms^{-1}, $\tau_e = 10$ eV, $Z = 7$, $n_i = 6.3\times10^{24}$ m^{-3} and, assuming the carbon has been photoionized to form a plasma, $n_{i'} = 1.75\times10^{27}$ $\mathrm{m}^{-3} = n_e$ $(Z' = 1)$, then $\ln\Lambda_{ii'}$ is 6.96 and ϵ is 154 keV, giving $\tau_{ii'} = 2.03\times10^{-8}$ and a mean-free-path of the tungsten of 8 mm. Clearly no shock will form at the tungsten–carbon boundary, but interpenetration of the two species will occur. Such a process cannot be modeled by the standard fluid code. This mean-free-path will be reduced when the radial electric field E set up to yield an equal inward electron current flow is included. E is $\eta n_i Zev$ and for a $Z' = 1$ carbon plasma at 10 eV discussed above, η is 3.3×10^{-6} Ω-m and $E = 9.2\times10^6$ Vm^{-1} so that 154-keV tungsten ions will be slowed over 16 mm in the absence of ion–ion collisions. For these parameters, the resultant slowing down distance is 5.5 mm. The released

https://doi.org/10.1017/S0263034601193092 Published online by Cambridge University Press

energy will obviously raise the electron temperature and degree of ionization, which will only increase the effective mean-free-path.

In this model, the electric field is well below the Dreicer runaway electric field, so that a Spitzer resistivity is appropriate. A more extreme case was considered by Simnett and Haines (1990) to explain the emission of hard X rays at solar coronal footpoints due to 1-MeV ions (and accompanying electrons) impinging on the relatively dense, cold chromosphere. The incoming electrons are scattered by the chromospheric plasma and an electric field is set up to maintain this inward electron flow to neutralize the inward current. Some of these electrons can attain an energy approaching 1 MeV and emit hard X-ray bremsstrahlung. If, however, the ratio of the plasma to beam density is high enough or the temperature of the chromospheric plasma is increased, this plasma itself (like the above case) provides the neutralizing current; if the Dreicer condition for runaway is also not violated, no energetic electrons and no hard X rays are produced.

It should be stated, however, that if the interior material is un-ionized, the mean-free-path of the incoming tungsten ions might appear to be less than 1 μm. However in these collisions, carbon atoms will acquire about 10 keV and will ionize. However, it is likely that photoionization and early precursor plasma interaction will lead to the foam becoming an ionized plasma earlier.

A remark should be made about the nature of ion–ion collisions within the precursor plasma stream itself for densities in the range $>10^{-4}$ solid density. Assuming that the ion temperature is the same as the electron temperature, for the values given above (10–30 eV), it is found that the Debye length is less than the Landau parameter. Thus the ion plasmas are strongly coupled and binary ion–ion collisions dominate. This is not the case for the more energetic collisions between interpenetrating streams.

Last, in the area of laser-produced plasmas, the phenomenon of interpenetrating plasma streams has been studied experimentally and theoretically by Bosch *et al.* (1992) using aluminum and magnesium, with results consistent with the arguments here.

7. ANOMALOUS RESISTIVITY

When the drift velocity v_D $(=J/n_e e)$ of the current-carrying electron exceeds some critical velocity v_{crit}, which is typically of the order of the ion sound speed, C_s $(=\sqrt{[(Z_e T_e + T_i)/m_i]})$, some form of micro- or velocity-space-instability will be triggered. It will rapidly grow in time and saturate in amplitude. The resulting turbulent electrostatic or electromagnetic wave structure will interact with the drifting electrons, causing them to be scattered. This scattering can be much larger than that caused by Coulomb collisions with ions; hence an anomalous resistivity will be generated.

The microinstability that is generally thought to be the most relevant for the *z* pinches is the lower hybrid drift instability, because in the *z*-pinch configuration the current density and drift velocity are orthogonal to the magnetic field. Related to the lower hybrid instability is the modified two-stream instability studied earlier by Bunemen (1961) and Ashby and Paton (1967). Krall and Liewer (1971) derived the first linear, electrostatic kinetic model of the lower hybrid instability. Davidson and Gladd (1975) developed a quasi-linear model to find a value for the anomalous resistivity. Huba and Papadopoulos (1978) considered electron resonance broadening as a saturation mechanism especially in finite β plasmas. Particle simulations by Winske and Liewer (1978), in contrast, find that ion trapping is a saturating mechanism in the high drift velocity regime, while Davidson (1978) found current relaxation and plateau formation can cause saturation at low drift velocity.

Perhaps the two most important papers to yield in 2-D nonlinear modeling a value for the anomalous collision frequency at saturation are Drake *et al.* (1984) and Brackbill *et al.* (1984). The former considered nonlinear mode–mode coupling showing that energy is transferred from long-wavelength modes to short-wavelength modes which are damped. The anomalous collision frequency ν_{anom} so found from this model is

$$\nu_{anom} = 2.4(\omega_e \omega_i)^{1/2}(v_d/v_i)^2. \tag{20}$$

Here $(\omega_e \omega_i)^{1/2}$, where ω_e and ω_i are the cyclotron angular frequencies of the electrons and ions, respectively, is the lower hybrid resonance frequency, while v_D and v_i are the electron drift velocity and the ion thermal speed, respectively.

In contrast, Brackbill *et al.* (1984) employed a 2-D implicit particle-in-cell code VENUS with 90,000 ions and electrons, initially with a Harris equilibrium. This was fully electromagnetic with finite β. The suggested saturation mechanism was electron kinetic dissipation with wavelengths greater than the electron Larmor radius. The resulting anomalous collision frequency found in this numerical simulation differs from Eq. (20) and is

$$\nu_{anom} = \frac{C}{4\pi\beta_i}(\omega_e \omega_i)^{1/2}(v_d/v_i)^2, \tag{21}$$

where C is 0.13 to 0.38 and β_i is the ratio of ion pressure to magnetic pressure.

Before applying these results to the *z* pinch it is perhaps worthwhile to recall the basic physics underlying the lower hybrid resonance. Though the ion cyclotron frequency is present in the formula, the ions are, in fact, to a good approximation unmagnetized. Figure 3 illustrates how the lower hybrid resonant frequency arises when the ion plasma frequency is much higher. Consider a plane electrostatic wave propagating in the *z* direction. The unmagnetized ions will oscillate to and fro in the $\pm\boldsymbol{z}$ direction. With a steady magnetic field in the $\boldsymbol{y}$ direction the magnetized electrons will have an oscillatory E/B drift in the $\pm\boldsymbol{x}$ direction. Superposed on this is the polarization drift, $E/(B\omega_{ce})$ in the $\pm\boldsymbol{z}$ direction that will convert the electron guiding center tra-

https://doi.org/10.1017/S0263034601193092 Published online by Cambridge University Press

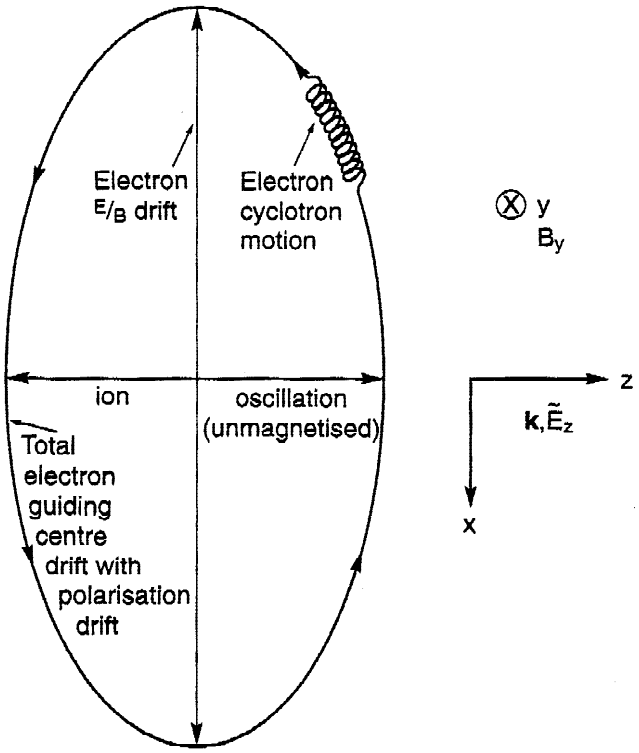

Fig. 3. Orbits of oscillating ions and guiding-center electrons, showing equal amplitude in the *Z*-direction at the lower hybrid resonance.

jectory into an ellipse. The resonance occurs, that is, a tendency for zero charge separation, when the spatial amplitude of the ion oscillation $eE/m_i\omega^2$ is equal to the width of the ellipse $E/(B\omega_{ce})$; this gives $\omega = (\omega_{ce}\omega_{ci})^{1/2}$.

The lower hybrid instability arises when a density gradient is present in the $-\boldsymbol{x}$ direction; then the electron elliptic motion leads to an increase of positive potential and charge at the positive peak of the wave and a similar amplification of the negative charge at the negative potential peak. The density gradient corresponds to a net diamagnetic drift of electrons in the $-\boldsymbol{z}$ direction. Hence such a current is responsible for the growth in the wave amplitude.

It is to be noted that nearly all the simulations and theory have been undertaken for a collisionless plasma. However the coronal plasma around each wire of a wire array is typically so collisional that the Hall parameter $\omega_e\tau_{ei}$ is less than unity. This is also true for single wires, and it is only in the very low-density outer corona that the Hall parameter is large enough to be able to apply these models of lower hybrid turbulence. However it is very useful (see Chittenden, 1995; Chittenden *et al.*, 1999) to apply such an anomalous collision frequency as one approaches the plasma–vacuum boundary. This anomalous collision frequency leads to a more realistic reduction of current density, and, in particular, a nonsingular electron drift velocity as the density approaches zero (or the value ascribed to the vacuum).

When modeling the magneto-Rayleigh–Taylor instability in the *r*–*z* plane (e.g., Peterson *et al.*, 1999; Douglas *et al.*, 2000), the inward moving bubbles of plasma leave behind extended spikes. A current reconnection across these spikes in the lower density "vacuum" would generate lower hybrid turbulence; it is doubtful whether the large anomalous resistivity would permit much current to flow despite the low inductance path. This is an active area of research. Indeed current reconnection is an intrinsic feature of the model proposed by Rudakov *et al.* (2000) to explain the dissipation of magnetic energy at stagnation.

Introduction of lower hybrid anomalous resistivity will change the formula for the Pease–Braginskii current, a point followed up by Robson (1989).

In the next section, anomalous resistivity will be introduced in a new model of disruption when gaps of low-density plasma exist between density islands at the time of an $m = 0$ disruption and thereafter.

It is to be hoped that with the new generation of computers, further work, perhaps in 3-D full electromagnetic, will be undertaken on lower hybrid turbulence, and the related modified two stream instability.

Meanwhile, attention could be drawn also to the need for better-diagnosed experiments. A recent paper by Takeda and Inuzuka (2000) presents measurements of anomalous resistivity associated with large amplitude noise at the lower hybrid frequency. Here the ratio v_D/v_i was large ($\sim 10^2$) and the anomalous collision frequency was essentially ω_e. This leads to Bohm diffusion. It is perhaps permissible to speculate that the formula for ν_{anom} given by Eq. (20) is only valid up to a value of ω_e, when it becomes independent of (v_D/v_i). For a hydrogen plasma, this will occur at v_D/v_i equal to 4.2.

8. DISRUPTIONS

During the nonlinear evolution of the $m = 0$ instability of a stagnated *z* pinch or plasma focus employing deuterium as the working gas, a significant pulse of neutrons appears, typically a yield of up to 10^{12} neutrons (Bernard *et al.*, 1979; Maissonier & Rager, 1979). The origin of this has been a great source of debate and controversy that has still not been resolved. Several of the proposed mechanisms are kinetic in nature and, in this short review, will be the main focus of discussions.

Normally the principal pulse of neutrons at the time of $m = 0$ disruption is the second pulse (Schmidt & the Poseidon Team, 1983). The likely explanation of the first pulse is essentially kinetic in origin. It was first hinted at in Trubnikov's (1986) paper (Sect. 2.10) and developed more realistically by Deutch and Kies (1988). Here it is considered that there is a sheet current piston that compresses the plasma as the first pinch is formed. Unlike the snowplough model, it is postulated that the ions, on encountering this moving piston, are effectively reflected by it and effectively are kicked inwards (by the radial electric field in the current sheet) with twice the velocity of the piston. It is then assumed that they are essentially collisionless and also conserve their angular momentum (a point made by Trubnikov, 1986, and earlier by Haines, 1983). On encountering the moving piston a second time, there is another gain of energy; indeed the

https://doi.org/10.1017/S0263034601193092 Published online by Cambridge University Press

faster ions have more reflections and gain more energy, a feature of this Fermi acceleration mechanism. There will be, as a result, a high energy ion tail and ion–ion collisions that will grow in number when the piston reaches close to the axis and will also yield D–D nuclear reactions, but of a superthermal nature. If the incoming piston is conical in shape, it will also lead to a growth in axial motion. It should be noted that multiple collisions of essentially collisionless ions are needed for this, a condition that might pertain in certain conditions in the precursor plasma of an imploding wire array.

Four important features of the principal pulse of neutrons are (i) it originates at the time of $m = 0$ instability, a point confirmed experimentally by Bernard *et al.* (1979); (ii) the neutrons have an anisotropic distribution consistent with originating from an ion beam in the *z*-direction (the direction of ion current, also confirmed by Bernard who employed a deuterated target on axis to verify this point); (iii) there is an associated relativistic electron beam traveling towards the anode (verified by measurements in a hollow anode by Nardi *et al.*, 1979); and (iv) there is a voltage spike and drop in the current.

Dealing briefly with the fluid models, Anderson *et al.* (1958) pointed out that at the time of necking off of the $m = 0$ instability, there is a large transient increase in inductance and associated electric field. In turn this electric field will accelerate the ions leading to an energetic ion beam and, by collisions, neutrons. The argument was based on ideal MHD, and as pointed out by Haines (1983), in the moving plasma the electric field as seen by the ions ($\mathbf{E} \times \boldsymbol{v} \times \mathbf{B}$) is zero. Furthermore it was shown that there is up-down (or $\pm \boldsymbol{z}$) symmetry each side of a neck, even for resistive MHD, so that if any ion jets occur from the necked region, they will occur equally in both directions. It requires introduction of the Hall term and, or, the finite ion-Larmor radius terms in the stress tensor to break this symmetry and allow a beam to form (Haines, 1983). Filippov (1979) proposed a moving boiler mechanism to explain the experimental results, a mechanism closest perhaps to that proposed by Vikhrev (1986). He claims that dense hot thermonuclear plasma is formed in the necks of an $m = 0$ instability, and bases this on 2-D MHD simulations. This is at variance with experimental measurements of *z* pinches, especially fiber pinches (Mitchell *et al.*, 1998), though Kassapakis (2000) has shown in a 2-D simulation that a suitable initial finite amplitude $m = 0$ deformation can lead to high density and temperature in a neck. Yan'kov (1991) proposed a propagating burning thermonuclear wave triggered by ignition at the $m = 0$ neck.

One of the difficulties in a kinetic model to give ion beams is to obtain consistency with overall conservation of a momentum; the question "where is the equal and opposite axial momentum deposited?" needs to be answered. A simple electrostatic model of a diode relies on a breakdown of quasi-neutrality so that the net charge density q_v provides a force per unit volume $q_v\mathbf{E}$ in an electric field. Because of Maxwell's equation this force is $\epsilon_0 \mathbf{E}\nabla\cdot\mathbf{E}$. To explain the Bernard *et al.* (1979) experiments where 1.9 MA of deuteron current of energy 300 keV was generated, it would require an outrageous electric field of over 10^{11} Vm^{-1}. The equal and opposite force would occur where the corresponding negative charge is situated. Indeed in one dimension,

$$\epsilon_0 E_z \partial E_z/\partial z = \frac{\partial}{\partial z}\left(\frac{1}{2}\epsilon_0 E_z^2\right)$$

will clearly integrate to zero across any double layer, showing that there is no net momentum transfer. A more realistic sheath acceleration was proposed by Haines (1981, 1983); but this was confined to the anode sheath, in which a radially inward E_z/B_θ drift of magnetized electrons would constitute the necessary $J_r B_\theta$ force, while the ions accelerated in the E_z field. The sheath thickness would lie between the Larmor radii of the electron and ion. The electrons on reaching the axis would exit axially through a hole in the anode. The equal and opposite force is transmitted to the anode itself through the magnetic pressure. It is difficult to see how such a mechanism could operate in an $m = 0$ neck in the main plasma column.

Haines (1983) proposed a model based on finite ion-Larmor-radius effects. Without an $m = 0$ perturbation, a collisionless pinch has ion trajectories that are singular or betatron-like with one Larmor radius of the axis with a guiding center flow in the opposite direction off-axis and, through diamagnetism, a net center of mass velocity of zero (see Sect. 3). During a dynamic creation of an $m = 0$ neck, a large amount of energy is given to the ions in this region, leading to a beam of energetic singular ions proceeding towards the cathode, and, off-axis, an equal and opposite momentum in guiding-center ions. These ions are more numerous, and so the energy change in these is much smaller than in the beam. Nevertheless, Tiseanu and Mandache (1994) have inferred such ions from measurements.

If the line density drops to a low value in the necked region, the drift parameter (e.g., the ratio of the electron drift velocity to the ion sound speed) increases past a critical value leading to the onset of microturbulence. Ryutov *et al.* (2000) discuss the onset of this, and the subsequent formation of a high energy ion tail as proposed by Vekstein and Sagdeev (1970). However the problem here is that the energetic ion tail evolves in the direction of the electron flow; on the contrary the ion beam that produces the neutrons flows in the opposite direction. The fraction of ions involved is $(m_e/m_i)^{1/4}$ and the opposite momentum is transferred to the remaining majority ions.

Trubnikov (1986) considered the sudden onset of microturbulence in the neck of the unstable *z* pinch (indeed the Buneman two-stream instability). Keeping the total current constant, he postulated a rapid transfer of this current to a peripheral plasma. The drop in inductance leads to a high voltage across this, and he considers furthermore that the peripheral plasma has a dielectric constant of $(c/V_A)^2$ where c is the velocity of light and V_A is the Alfvén velocity. The

https://doi.org/10.1017/S0263034601193092 Published online by Cambridge University Press

ions in the peripheral plasma get accelerated in the high transient electric field by diode action and subsequently impact the adjacent dense plasma to produce neutrons.

While there are difficulties over conserving the total momentum, the large electric fields needed for diode action and the concept of a dielectric under these conditions, there are some interesting and useful features for a more refined model. It can be shown that when the line density N of a z pinch drops below a critical value N_c based on the Bennett relation,

$$16\pi NK_BT = \mu_0 I^2 \tag{22}$$

when $I = NeC_s$ and $C_s^2 = k_BT/m_i$, giving $N_c = (16\pi/\mu_0) \times (m_i/e^2)$, it is impossible for a pressure balance to occur if the drift velocity is unable to exceed C_s because of microturbulence. Thus in the necked region, while earlier the large ion-Larmor radius acceleration scheme might apply at first, as N drops, a runaway electron current and microturbulence will occur. The plasma in this region will heat up by this anomalous resistance and not be confined, but expand radially. Likewise this will lead to a redistribution of current in a time of order 50 ps and a reversal of axial electric field E_z is possible at larger radii ($\partial B_\theta/\partial t$ is large and negative and therefore so is $\partial E_z/\partial r$). The ion acceleration that could occur will be in one direction near the axis and in the opposite at larger radii, thereby allowing axial momentum to be conserved. The electron current in the Z direction will be driven between these plasma density islands by a large $v_r B_\theta$ electric field, this situation then continuing in the benign decaying phase after the disruption (Beg *et al.*, 1997). More work needs to be done on the theory and also on more experimental diagnosis of turbulence, current distribution, and electron temperature in the low-density region before there is an understanding of this phase of the z pinch.

REFERENCES

Aivazov, I.K. *et al.* (1988). *Sov. J. Plasma Phys.* **14**, 110.
Anderson, O.A. *et al.* (1958). *Phys. Rev.* **109**, 612.
Arber, T.D. (1996). *Phys. Rev. Lett.* **77**, 1766.
Arber, T.D. *et al.* (1994). *Phys. Rev. Lett.* **72**, 2399.
Arber, T.D. *et al.* (1995). *Phys. Rev. Lett.* **74**, 2698.
Ashby, D.E.T.F. & Paton (1967). *Plasma Phys.* **6**, 254.
Beg, F.N. *et al.* (1997). *Plasma Phys. Controlled Fusion* **39**, 1.
Bell, A.R. *et al.* (1981). *Phys. Rev. Lett* **46**, 243.
Bernard, A. *et al.* (1979). *Plasma Physics and Controlled Nuclear Fusion Research (1978)*, Vol. 2, p. 159. Vienna: IAEA.
Bosch, R.A. *et al.* (1992). *Phys. Fluids* **B4**, 979.
Brackbill, J.U. *et al.* (1984). *Phys. Fluids* **27**, 2682.
Braginskii, S.J. (1958). *Zh. Eksp. Teor. Fiz.* **33**, 459 [*1958 Sov. Phys. JETP* **6**, 358].
Buneman, O. (1961). *Technical Report No. 251-1*, Air Force contract **AF49**, pp. 638–660. Stanford, CA: Electron Devices Laboratory.
Chittenden, J.P. (1995). *Phys. Plasmas* **2**, 1242.
Chittenden, J.P. & Haines, M.G. (1993). *J. Phys. D* **26**, 1048.
Chittenden, J.P. *et al.* (1999). *Phys. Rev. Lett.* **83**, 100.
Davidson, R.C. & Gladd, N.T. (1975). *Phys. Fluids* **18**, 1327.
Davidson, R.C. (1978). *Phys. Fluids* **21**, 1375.
Davies, H.M., Dangor, A.E., Coppins, M. & Haines, M.G. (2001). *Phys. Rev. Lett.* (in press).
Deutch, R. & Kies, W. (1988). *Plasma Phys. Controlled Fusion* **30**, 921.
Drake, J.F. *et al.* (1984). *Phys. Fluids* **27**, 1148.
Dreicer, H. (1960). *Phys. Rev.* **117**, 329.
Douglas, M.R. *et al.* (2000). *Phys. Plasmas* **7**, 1935.
Epperlein, E.M. & Haines, M.G. (1986). *Phys. Fluids* **29**, 1029.
Filippov, N.V. (1979). *Sov. Phys. JETP* **49**, 785.
Haines, M.G. (1978). *J. Phys. D* **11**, 1709.
Haines, M.G. (1981). *Philos. Trans. R. Soc. London* **A300**, 649.
Haines, M.G. (1983). *Nucl. Instrum. Methods* **207**, 179.
Haines, M.G. (1992). Non-local Effects in Laser Plasmas, *Spatial Dispersion in Solids & Plasmas* (Halevi, P. Ed.). Amsterdam: Elsevier Science Publ.
Haines, M.G. (1996). *Plasma Phys. Controlled Fusion* **38**, 897.
Haines, M.G. & Coppins, M. (1991). *Phys. Rev. Lett.* **66**, 1462.
Haines, M.G. *et al.* (1990). *J. Plasma Phys. and Controlled Nucl. Fusion Research*, Vol. 2, p. 769. Vienna: IAEA.
Holstein, P.A. *et al.* (1986). *J. Appl. Phys.* **60**, 2296.
Huba, J.D. & Papadopoulos, K. (1978). *Phys. Fluids* **21**, 121.
Johnston, T.W. (1960). *Phys. Rev.* **120**, 1103.
Kassapakis, N. (2000). Ph.D. Thesis, University of London.
Krall, N.A. & Liewer, P.C. (1971). *Phys. Rev.* **A4**, 2094.
Lebedev, S.V. *et al.* (1999). *Phys. Plasmas* **6**, 2016.
Maissonier, Ch. & Rager, J.P. (1979). *Proc. Third Int. Conf. High Power Electron and Ion Beam Research and Technology*, Novosibirsk, USSR, Vol. 1, p. 233. Novosibirsk: Institute of Nuclear Physics.
Matzen, M.K. (1997). *Phys. Plasmas* **4**, 1519.
Mitchell, I.H. *et al.* (1998). *IEEE Trans. Plasma Sci.* **26**, 1269.
Nardi, V. *et al.* (1979). *Plasma Physics and Controlled Nuclear Fusion Research (1978)*, Vol. 2, p. 143. Vienna: IAEA.
Peterson, D.L. *et al.* (1999). *Phys. Plasmas* **6**, 2178.
Robson, A.E. (1989). *Phys. Rev. Lett.* **63**, 2816.
Rudakov, L.I. *et al.* (2000). *Phys. Rev. Lett.* **84**, 3326.
Ryutov, D.D. *et al.* (2000). *Rev. Mod. Phys.* **72**, 167.
Schmidt, H. & Poseidon Team (1983). *Proc. Third Int. Workshop on Plasma Focus Research*, Stuttgart, p. 107.
Shvarts, D. *et al.* (1981). *Phys. Rev. Lett.* **47**, 247.
Simnett, G.M. & Haines, M.G. (1990). *Solar Phys.* **130**, 253.
Spitzer, L. & Härm, R. (1953). *Phys. Rev.* **89**, 977.
Takeda, Y. & Inuzuka, H. (2000). *Phys. Letters* **A265**, 282.
Tiseanu, I. & Mandache, N. (1994). *Dense Z-Pinches*. AIP Conference Proceedings, Vol. 299, p. 356.
Trubnikov, B.A. (1986). *Sov. J. Plasma Phys.* **12**, 271.
Vekshtein, G.E. & Sagdeev, R.Z. (1970). *JETP Lett.* **9**, 194.
Vikhrev, V.V. (1986). *Sov. J. Plasma Phys.* **12**, 262.
Winske, D. & Liewer, P.C. (1978). *Phys. Fluids* **21**, 1017.
Yan'kov, V.V. (1991). *Sov. J. Plasma Phys.* **17**, 305.